Applied and Environmental Microbiology, Feb. 2011, p. 1041–1048 Vol. 77, No. 3
0099-2240/11/$12.00 doi:10.1128/AEM.02068-10

Bacterial Colonization of Pellet Softening Reactors Used during Drinking Water Treatment[▽]

Frederik Hammes,[1]* Nico Boon,[2] Marius Vital,[1] Petra Ross,[3] Aleksandra Magic-Knezev,[4] and Marco Dignum[5]

Eawag, Swiss Federal Institute of Aquatic Science and Technology, Dübendorf, Switzerland[1]; Laboratory of Microbial Ecology and Technology (LabMET), Ghent University, Ghent, Belgium[2]; and Delft University of Technology, P.O. Box 5048, 2600 GA Delft,[3] Het Waterlaboratorium (HWL), J. W. Lucasweg 2, 2031 BE Haarlem,[4] and Waternet, P.O. Box 8169, 1005 AD Amsterdam,[5] Netherlands

Received 1 September 2010/Accepted 29 November 2010

Pellet softening reactors are used in centralized and decentralized drinking water treatment plants for the removal of calcium (hardness) through chemically induced precipitation of calcite. This is accomplished in fluidized pellet reactors, where a strong base is added to the influent to increase the pH and facilitate the process of precipitation on an added seeding material. Here we describe for the first time the opportunistic bacterial colonization of the calcite pellets in a full-scale pellet softening reactor and the functional contribution of these colonizing bacteria to the overall drinking water treatment process. ATP analysis, advanced microscopy, and community fingerprinting with denaturing gradient gel electrophoretic (DGGE) analysis were used to characterize the biomass on the pellets, while assimilable organic carbon (AOC), dissolved organic carbon, and flow cytometric analysis were used to characterize the impact of the biological processes on drinking water quality. The data revealed pellet colonization at concentrations in excess of 500 ng of ATP/g of pellet and reactor biomass concentrations as high as 220 mg of ATP/m^3 of reactor, comprising a wide variety of different microorganisms. These organisms removed as much as 60% of AOC from the water during treatment, thus contributing toward the biological stabilization of the drinking water. Notably, only a small fraction (about 60,000 cells/ml) of the bacteria in the reactors was released into the effluent under normal conditions, while the majority of the bacteria colonizing the pellets were captured in the calcite structures of the pellets and were removed as a reusable product.

High calcium and magnesium concentrations in municipal drinking water (also called "hardness") have adverse esthetic and economic implications, such as scale deposits in water boilers, a higher demand for detergents in washing machines, and enhanced copper and lead release from pipe materials in drinking water distribution systems (5, 9, 22). As a result, some countries have specific hardness standards for finished drinking water (typically about 150 mg/liter as $CaCO_3$). In regions where hardness is problematic and calcium concentrations exceed guideline values, waterworks have implemented centralized softening during the treatment process (9, 15).

The concept of centralized drinking water softening was first proposed half a century ago in the Netherlands and was developed practically into upflow pellet softening (PS) reactors at the Amsterdam Water Supply (9). PS reactors are also described in the literature as fluidized pellet reactors (15) or fluidized-bed crystallization columns (5, 13). Both the process and operational descriptions for these systems are provided in detail elsewhere (27, 28, 31). Briefly, PS reactors are fluidized pellet reactors with a high upflow velocity (60 to 90 m/h) where seeding material (e.g., Garnet sand) with a small grain size (diameter, 0.15 to 0.4 mm), providing a large crystallization area, is dosed on a regular basis. A basic chemical, such as caustic soda, soda ash, or lime, is added at the bottom of the reactor (influent), raising the pH (above pH 9) and thereby facilitating the crystallization of calcium carbonate ($CaCO_3$; calcite) on the seeding material. The precipitation of calcite on the seeding material leads to gradually increasing pellet sizes, allowing the larger pellets to progress toward the lower levels of the reactor. Pellets have a typical residence time of about 100 days in the reactor; they are then removed regularly from the bottom of the reactor and are reused in other industrial processes, such as the steel or chicken-farming industry (28, 31). While the positions of PS reactors in a drinking water treatment train can differ, one approach is to place them directly after ozonation systems (6, 13, 31), followed by membrane filtration (15), sand filtration (6), or granular active carbon (GAC) filtration (13, 31).

Pellet reactors have as their main purpose the softening of water by means of chemically driven crystallization of calcium as calcite. Hence, these reactors are normally not designed, analyzed, or considered from a microbiological perspective. On the one hand, this is not surprising, given that the short hydraulic retention time (5 min), high initial pH (>9), and, in some cases, aggressive oxidative pretreatment (ozonation) would be regarded as unfavorable for the presence and growth of microorganisms in these reactors. On the other hand, the placement of PS reactors directly after an ozonation treatment exposes the reactors to an increased content of easily degradable organic carbon (34), which is likely to stimulate bacterial growth. Moreover, it is common knowledge that most granulated filter materials that come into contact with drinking water (e.g., sand, anthracite, and active carbon) sooner or later become colonized by a variety of indigenous bacteria (16, 32). Notably, the bacteria colonizing such materials are not merely

* Corresponding author. Mailing address: Eawag, Swiss Federal Institute of Aquatic Science and Technology, CH-8600 Dübendorf, Switzerland. Phone: 41 44 823 5160. Fax: 41 44 823 5547. E-mail: frederik.hammes@eawag.ch.

▽ Published ahead of print on 10 December 2010.

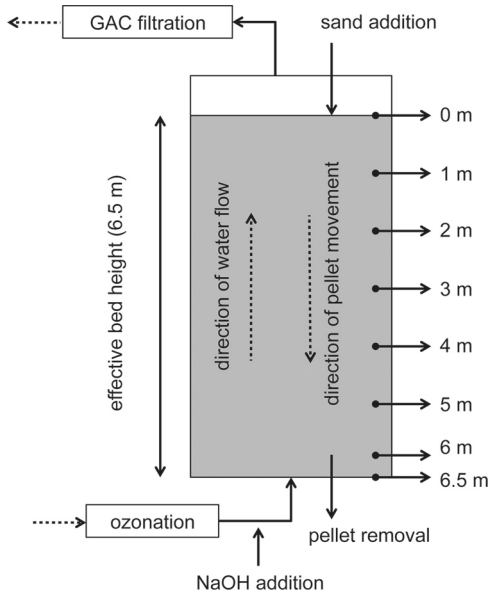

FIG. 1. Schematic presentation of the layout, sampling points, and position in the treatment train of the full-scale "Amsterdam-type" PS reactor analyzed in the present study (based on references 28 and 29).

opportunistic but perform an essential biofiltration function in the treatment process through the removal of biodegradable organic matter (12, 25, 32).

To the best of our knowledge, there is currently no information on bacterial colonization of PS reactors. The purpose of this study was, therefore, to quantify and characterize the microbial biomass in a full-scale PS reactor as a first step toward understanding the function and consequences of these opportunistic microorganisms in the drinking water treatment process.

MATERIALS AND METHODS

Reactor configuration and sampling. Water samples and pellets were collected from the treatment plant of Leiduin, Netherlands. The treatment train comprises (i) rapid sand filtration, (ii) ozonation, (iii) pellet softening, (iv) biologically activated carbon (BAC)/GAC filtration, and (v) slow sand filtration. The PS reactor was an "Amsterdam-type" upflow fluidized sand bed reactor (31) (Fig. 1). More operational details, including photographs of the full-scale PS reactors that were sampled in the present study, can be found elsewhere (9, 27, 28). Water samples were collected in carbon-free glassware before and after residence in the reactor. Pellets were collected from different heights (every 1 m) of the reactor using gravity suction with a marked hosepipe, where 0 m is the top of the actual reactor bed height, and 6.5 m is the bottom of the reactor (Fig. 1). All samples were analyzed within 4 h of sampling. In addition to all other analyses, the pellet concentration (dry weight/volume) for each sample was determined, and the size of pellets from each level was measured by light microscopy of a minimum of 50 particles. Changes in the concentration of calcium, the pH, and the pellet size were additionally modeled for the specific day of sampling by using the mathematical models described in detail elsewhere (30).

Determination of the amount of active biomass on the pellets. The amount of biomass on the pellets was measured by ATP analysis using an optimized version of the method described by Velten and coworkers (32). Briefly, 10 g of the sand/pellets was rinsed gently three times with 100 ml filtered (pore size, 0.22 μm) nonchlorinated tap water. Thereafter, 200 mg of the rinsed material was placed in a sterile Eppendorf tube and was submerged in 100 μl of sterile nonchlorinated tap water. Three hundred microliters of a commercial ATP reagent (BacTiter-Glo microbial cell viability assay; Promega, Madison, WI) was then added, and the sample was incubated with gentle shaking at room temperature. After 2.5 min of incubation, the luminescence (expressed as relative light units) was measured on a luminometer (GloMax 20/20; Turner BioSystems), and the results were converted to ATP concentrations by means of a calibration curve prepared with pure ATP and heat-sterilized pellets. After analysis, the pellets were dried (at 90°C for 24 h); the dry weight was determined; and the ATP data were normalized to the dry weight. All samples were analyzed in triplicate.

Microscopic evaluation of the pellets. Pellet samples were fixed with formaldehyde (2.5%; 1 h), washed (with filtered tap water), and stained (4 h; dark incubation) with SYBR Gold nucleic acid stain (1,000-fold diluted stock solution; Invitrogen, Switzerland). Staining was followed by a six-step dehydration with a glycerol-water gradient (40 to 100%) with 30 min per step. The dehydration was carried out to increase the image resolution when glycerol objectives were used. Confocal laser scanning microscopy (CLSM) images were captured with a Leica SP5 microscope as described previously (19). SYBR Gold was excited at 488 nm, and emission was detected at 503 to 553 nm. Autofluorescence of calcite was excited at 405 nm and detected at 406 to 459 nm. Three-dimensional depth stacks were captured at distances between 100 and 200 μm with 1-μm steps and were subsequently reconstructed with Imaris software (Bitplane Scientific Software, Zurich, Switzerland). For scanning electron microscopy (SEM), the fixed samples (as described above) were first serially dehydrated with ethanol at concentrations up to 100%, then dried at the critical point, and thereafter sputter-coated with a 10-nm layer of gold.

Fluorescent staining and FCM of water samples. Staining for intact cell counts and flow cytometry (FCM) were carried out as described previously (11, 2). Briefly, for a working solution, SYBR Green I (SG) (Invitrogen AG, Basel, Switzerland) was diluted 100× in anhydrous dimethyl sulfoxide (DMSO), and propidium iodide (PI; 30 mM) was mixed with the SYBR Green I working solution at a ratio of 1:50 (SGPI). This working solution was stored at −20°C until use. From every water sample, 1 ml was stained with SGPI at 10 μl/ml. Before analysis, samples were incubated in the dark for 15 min. Prior to flow cytometric analysis, the water samples were diluted with filtered (pore size, 0.22 μm) commercially available bottled water (Evian, France) to 10% (vol/vol) of the initial concentration. FCM was performed using a Partec CyFlow SL instrument (Partec GmbH, Münster, Germany) equipped with a blue 25-mW solid-state laser emitting light at a fixed wavelength of 488 nm. Green fluorescence was collected at 520 ± 10 nm; red fluorescence, above 630 nm; and high-angle sideward scatter (SSC), at 488 nm. The trigger was set on the green fluorescence channel, and data were acquired on two-parameter dot plots; no compensation was used for any of the measurements. The CyFlow SL instrument is equipped with volumetric counting hardware and has an experimentally determined quantification limit of 1,000 cells/ml (11).

HPC analysis of water samples. The heterotrophic plate count (HPC) method was used according to the Dutch guidelines for drinking water (NEN-EN-ISO 6222). Briefly, 1 ml of the water sample was transferred to a sterile petri dish and was mixed with about 15 ml plate count agar (PCA; Oxoid, Cambridge, United Kingdom). The agar was kept at 42°C until use. The plates were incubated at 22°C for 68 ± 4 h and were then manually counted.

DGGE of the pellets. DNA was extracted according to the method of Boon et al. (4). One microliter of the extracted DNA was amplified by PCR with the bacterium-specific 16S rRNA forward primer 338f and the reverse primer 518r (3, 18). PCR products were subjected to denaturing gradient gel electrophoresis (DGGE) as described previously (3). Cluster analysis (Ward algorithm) of the DGGE patterns was performed with Bionumerics software (version 2.0; Applied Maths, Kortrijk, Belgium). The calculation of the similarities is based on the Pearson correlation coefficient and results in a distance matrix. Ecological interpretation of the molecular data was conducted as reported by Marzorati et al. (17).

Dissolved organic carbon (DOC) and AOC. The concentration of assimilable organic carbon (AOC) was determined by a batch growth assay as described previously (12). Briefly, the pasteurized and filtered water samples (15 ml) were inoculated with 50 μl (initial concentration in the assay, 1×10^4 cells/ml) of a bacterial AOC test inoculum. These suspensions were then incubated at 30°C for 3 days (until stationary phase was reached), and the resulting growth was measured by flow cytometry (see above). The AOC test inoculum comprised indigenous drinking water communities obtained by mixing 50% bottled mineral water and 50% nonchlorinated tap water. The AOC concentration (in micrograms per liter) was estimated from final cell concentrations (number of cells per milliliter) by using a theoretical conversion factor (1 μg AOC = 10^7 cells) (12). All assays were performed in triplicate, and the detection limit of the method was 10 μg/liter.

Reactor modeling (calcium concentration, pH, and pellet size). For the determination of the amount of calcium, the pH, and the pellet sizes at different heights in the reactor on the sampling days, mathematical models were used as described by van Schagen et al. (30). Briefly, the model consists of three parts:

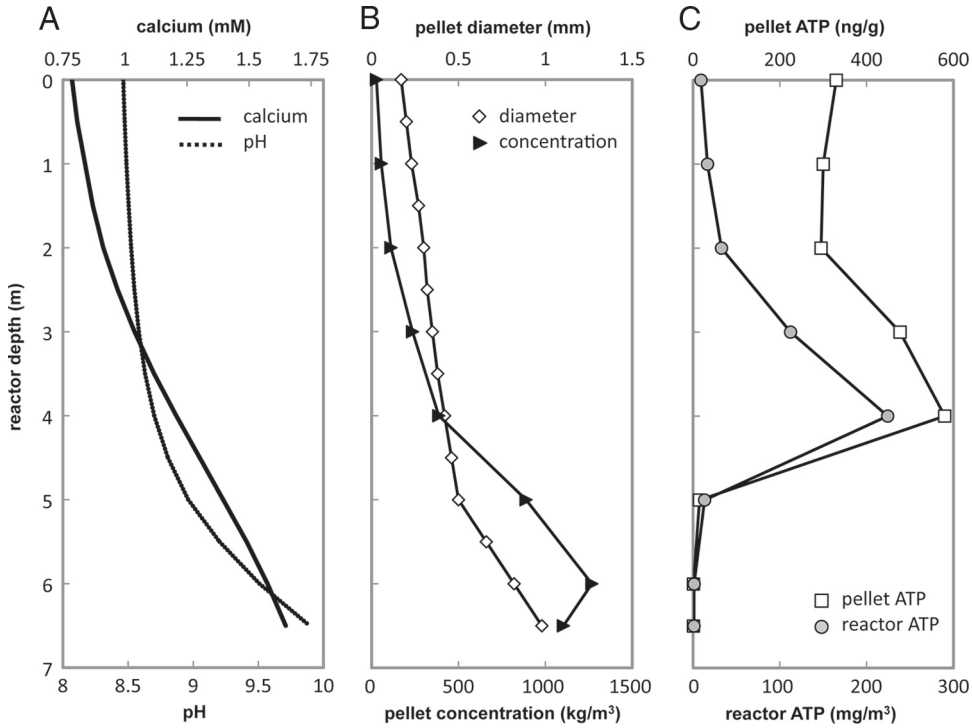

FIG. 2. Changes in the main reactor parameters over the sampling depth. (A) Modeled decreases in calcium concentrations (mM) and pH. (B) Measured changes in pellet diameter (mm) and concentration in the reactor (kg of pellets/m^3 of reactor). (C) ATP concentrations measured in triplicate on the pellets (ng of ATP/g of pellets) and effective ATP concentration in the reactor (mg of ATP/m^3 of reactor).

the calcium carbonic acid equilibrium, the fluidization of the bed to determine the available crystallization surface in the reactor, and the modeling of the crystallization rate based on the crystallization surface and the calcium carbonic acid equilibrium.

RESULTS AND DISCUSSION

Calcium removal and pellet formation. The influent of the analyzed PS reactor is naturally high in calcium (1.74 mM) and alkaline (pH 9.7) due to the continuous dosing of caustic soda (Fig. 1 and 2A). These conditions, in combination with the seeding material, drive the main process of the PS reactors, namely, the removal of calcium through crystallization as calcite on the pellet surfaces. The process is controlled on a daily basis through online monitoring and modeling (29, 30). The pH and calcium data (Fig. 2A) were modeled based on measurements of the bed height, pellet size, and pellet concentration (Fig. 2B). Note that the reactor was partitioned and was sampled from top (actual fluidized bed height) to bottom (Fig. 1), following the direction in which the grains/pellets progress through the reactor. From the modeled and measured data, it is evident that 75% of the calcite formation and crystallization occurred in the bottom section (the bottom 1.5 m) of the reactor (Fig. 2A). Apart from its primary purpose of calcium removal, the crystallization event has two main consequences for the system. First, the pH decreases (on the specific sampling day, from pH 9.7 to pH 8.1) due to a shift in the carbonate equilibrium (Fig. 2A) (10), rendering the water more favorable for heterotrophic microbial growth. Second, the calcite crystallizes on the pellet surfaces, resulting in a significant increase in the pellet size and thus the pellet concentration (kg of pellets/m^3 of reactor) in the lower section of the reactor; the average individual pellet volume increased 8-fold in the bottom 1.5 m of the reactor (Fig. 2B). As discussed below, the latter process has a considerable impact on the distribution of biomass on the pellets and throughout the reactor.

Biomass distribution through the PS reactor. Since ATP is the main transporter of chemical energy for metabolism within cells, ATP quantification can be used as a suitable cultivation-independent method for the description of active biomass in drinking water systems (16, 32). ATP analysis revealed a distinct distribution through the reactor (Fig. 2C). The smallest (and newest) grains at the top of the reactors had a high ATP concentration (330 ng of ATP/g of pellet). The active biomass concentration increased concomitantly with the size of the particles deeper in the reactor; the highest ATP concentration (580 ng of ATP/g of pellet) was detected at a depth of about 4 m (as measured from the top of the fluidized bed). These active biomass concentrations are similar to concentrations reported for conventional drinking water biofiltration systems. For example, Magic-Knezev and van der Kooij (16) reported concentrations of 12 to 60 ng of ATP/g of sand for slow sand filters and 11 to 1,728 ng of ATP/g of sand for rapid sand filters, while Velten et al. (32) reported values in the range of 20 to 2,000 ng of ATP/g of material for granular active carbon particles. This suggests that the biomass in the PS reactors is not just a low level of incidental bacterial contamination but rather represents a dynamic and actively growing biological system similar to those found in conventional drinking water biofilters. Moreover, the increased activity in the lower-middle section (at 4 m from the top) of the PS reactor points to a denser

colonization of these larger particles, since the surface-to-volume ratio of a spherical particle decreases with increasing volume of the particle. The effective reactor biomass concentration (mg of ATP/m^3 of reactor) depends on the active biomass concentration (ng of ATP/g of pellet) and the pellet concentration in the reactor (kg of pellets/m^3 of reactor). Since the pellet concentration increased significantly as a function of reactor depth (Fig. 2), the effective reactor biomass concentration increased considerably more than the concentration of ATP on the pellets (Fig. 2C). As a result, the lower-middle sections of the PS reactor had the highest concentrations of active biomass (220 mg of ATP/m^3 of reactor at 4 m [Fig. 2C]).

However, the trend for the biomass to increase with increasing reactor depth was not maintained. At a depth between 4 and 5 m, the ATP concentration decreased by 97% (to 15 ng of ATP/g of pellet), even though the pellet size and concentration increased more than 2-fold in the same section (Fig. 2). This striking decrease in the active biomass concentration can be attributed to the main calcite crystallization event and the concomitant pH change (Fig. 2A), which occurred in the bottom section of the reactor. First, the crystallization of calcite on the pellet surface physically encapsulated and trapped the bacteria in a dense crystalline layer (discussed below), which most probably resulted in cell death due to disruption of the proton motive force, coupled with nutrient limitation (23). Second, the higher pH in the bottom of the reactor is probably less favorable for the growth of bacteria than the lower pH values at the top of the reactor to which the bacteria were originally conditioned. The total reactor biomass, calculated from the reactor dimensions (Fig. 1) and the reactor biomass concentration (mg of ATP/m^3 of reactor) at each depth, gave an estimated amount of 2.9 g ATP for the entire reactor. Using the proposed ATP-to-biomass conversion value (1 g of ATP = 250 g of biomass) (14), this equates to a total reactor biomass of about 725 g. However, care should be taken with the interpretation of such conversions, since numerous factors affect cellular ATP concentrations, notably cell size, type, physiology, and activity. Nonetheless, this is a considerable amount of biomass, which can be sustained only through a continuous supply of biodegradable nutrients and which potentially influences the performance of the pellet reactor as well as that of downstream treatment processes. These issues are discussed in further detail below.

Microscopic examination of the pellets. Figure 3 shows representative SEM and CLSM images of grains/pellets from the PS reactor, demonstrating the series of main events occurring as the pellets progress downward through the reactor. Figure 3A shows a SEM image from the top of the reactor, at a depth of 1 m. At this depth, the original seeding material was still clearly visible but was already covered with irregular patches of unstructured amorphous calcium carbonate and biofilm. These first calcite precipitates increase the effective surface area of the particle, making it more susceptible to additional crystallization while creating a rough surface suitable for bacterial attachment and biofilm formation. It is plausible that bacteria also contribute to the crystallization process to some extent. It was reported previously that bacterial surfaces can serve as crystal nucleation sites for $CaCO_3$ formation (8), while their presence also expands the total surface area of the particle. This would contribute to an additional lowering of the saturation index (SI) for $CaCO_3$ crystallization. In this regard, van Dijk and Wilms have shown that the kinetics of heterogeneous nucleation of $CaCO_3$ are determined by (i) supersaturation and (ii) the specific surface area that is available (28). However, the degree to which the biomass in the PS reactors contributes to the calcite crystallization process has not been investigated in the present study.

At a depth of 4 m, characterized by the highest active biomass concentration, the seeding material was completely covered with an amorphous and highly porous layer of $CaCO_3$ (average thickness, 250 μm) (Fig. 3B). This porous structure creates a higher surface area on each pellet, which provides additional colonization area, partly explaining the higher ATP concentrations found in this section of the reactor (Fig. 2C). Filamentous bacteria were notably present in the reactor between the depths of 1 and 5 m. While the aggressive sample preparation required for SEM analysis has reduced some of the filaments to shorter stubs on the pellet surface (Fig. 3B), the actual nature of these filaments is particularly evident in stained, 3-dimensional CLSM images of fresh samples (Fig. 3C). In fact, the CLSM image provides strong visual confirmation of the intense colonization present on the pellets in the lower-middle section of the reactor (depth, 4 m), corroborating the ATP data shown in Fig. 2C. These pellets can clearly be regarded as biologically active particles, comparable to colonized particulate material found in conventional biofilters (e.g., BAC, GAC, and rapid sand filters).

Figure 3D shows a typical example of a large, smooth, spherical pellet from the bottom (depth, 6 m) of the PS reactor. At this stage, the main crystallization event (Fig. 2) has resulted in a dense layer (thickness, up to 600 μm) of crystalline calcite forming around the seeding grains (Fig. 3A) and calcite-biomass layers (Fig. 3B) of the pellets, resulting in a final product that is easily handled and has an economic value (28). Pellets were manually bisected in order to view their internal structure. In the bisected pellet (Fig. 3E), the main stages of crystallization are clearly discernible. In the center, the original seeding grain is evident (compare with Fig. 3A), surrounded by the amorphous biomass-calcite layer (Fig. 3B and C), and finally encrusted by the dense, crystalline calcite layer (Fig. 3D). This image clearly illustrates how the biomass present in the middle section of the reactor was completely encapsulated (and thus inactivated) by the precipitation process. The main advantage of this encapsulation is that the active biomass from the reactor is trapped in the calcareous layers and thus is easily removed from the treatment system together with the pellets. This supports the assertion by van Dijk and Wilms (28) that PS reactors can indeed be viewed as a truly "clean technology," associated with little or no waste product.

Community analysis. The purposes of the DGGE analysis were (i) to confirm the presence of bacteria in the PS reactors, (ii) to obtain information on the bacterial diversity in the reactor in general, and (iii) specifically to determine the distribution of bacteria over different reactor depths. Microbial community analysis by DGGE suggested the dominance of a large variety of bacterial strains through all depths of the reactor (Fig. 4). All the samples from depths of 1 to 4 m contained more than 30 bands and clustered with each other with high similarity (the overall similarity between all samples was 87.4% ± 8.1%, which is very high). At depths of 5 m and 6 m,

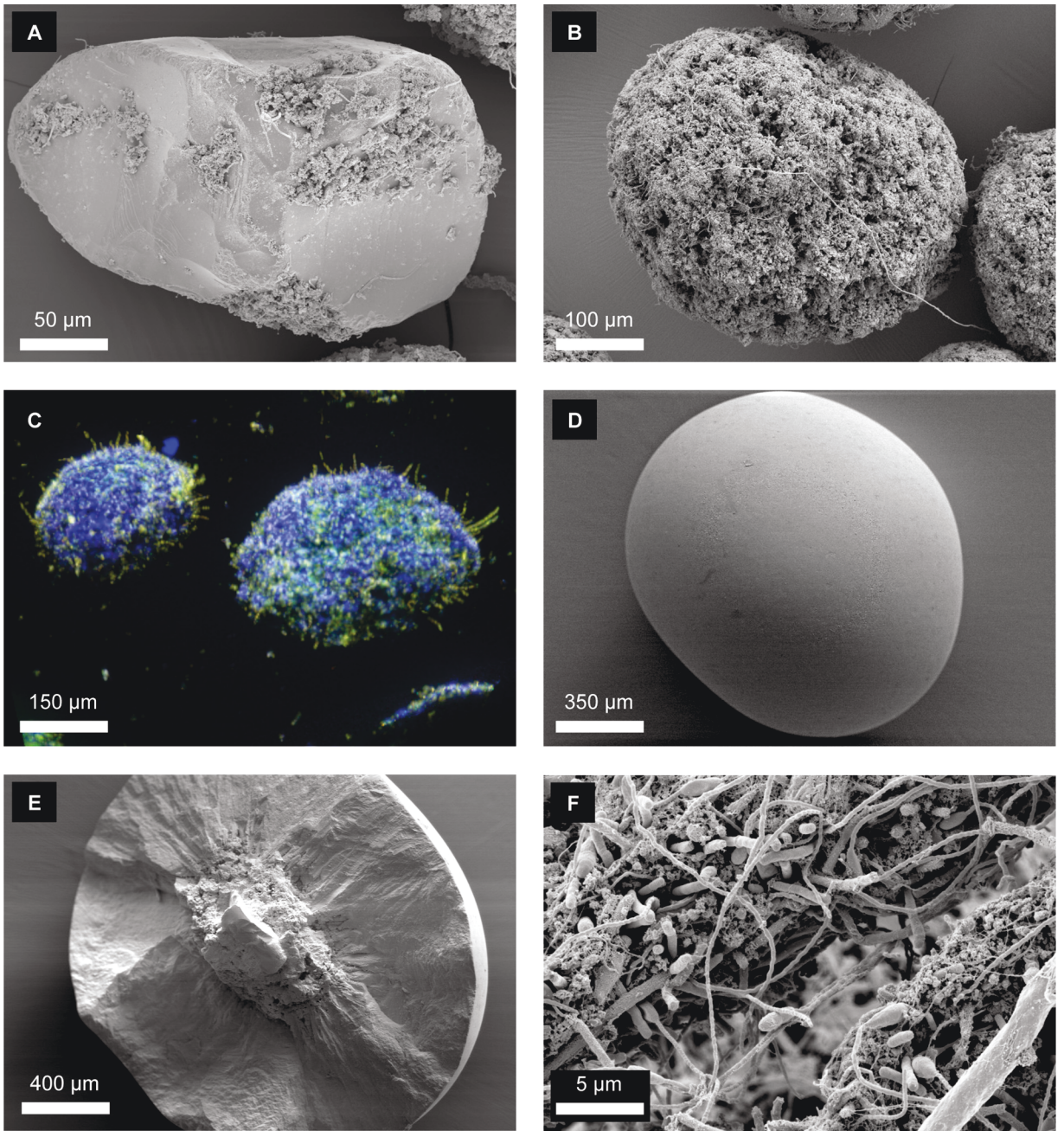

FIG. 3. Microscopic examination of the PS reactors. (A and B) SEM images from the top (depth, 1 m), showing patchy coverage of the seeding material with amorphous calcite and bacteria (A), and the lower-middle section (4 m), showing a porous calcite-bacterium matrix covering the entire surface of the seeding material (B). (C) Composite CLSM image (135 images) showing the presence of filamentous bacteria (green) on the surface of the calcium carbonate (blue). (D and E) SEM images from the bottom (6 m), showing large, smooth pellets (D), which, upon manual fracturing, reveal the original sand grain surrounded by the amorphous calcite-bacterium matrix and finally encrusted with a crystalline calcite layer (E). (F) SEM image of pellet material originating from a "disturbance layer" in a PS reactor, showing a calcareous biofilm characterized by extremely dense biomass of particularly long and/or filamentous bacteria.

the software recognized progressively fewer bands (21 and 25, respectively). However, this does not necessarily suggest lower diversity or a different community structure; the encapsulation of bacteria in the calcified pellet matrix (Fig. 3D and E) possibly restricted DNA extraction for molecular analysis. Nonetheless, calculation of the evenness (Gini values) and range-weighted richness (Rr) from the DGGE data (17) further suggested high similarity between the different samples. The Gini values (33) did not differ considerably between the samples (values between 0.36 and 0.44), showing that the community was moderately even throughout the reactor. The Rr values ranged from 47 to 161, with the highest values calculated for the upper half (depths of 1 to 4 m) of the reactor.

The similarities of the communities at the different depths of

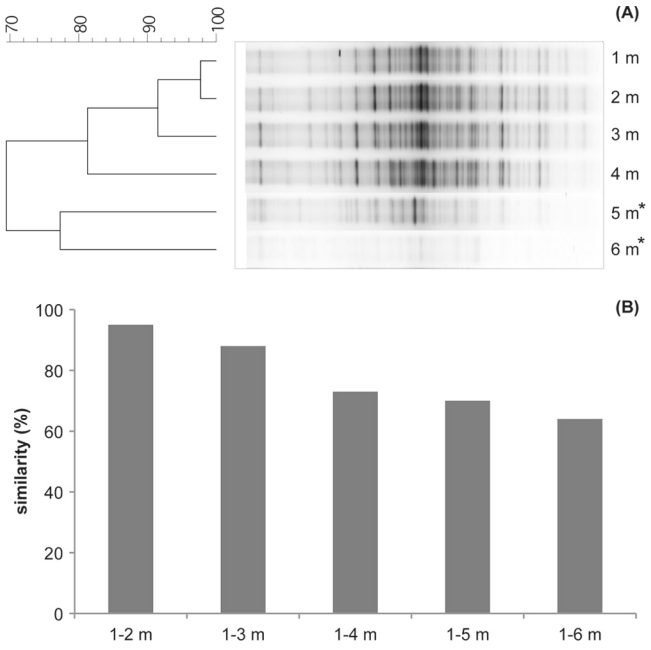

FIG. 4. (A) DGGE and cluster analysis of the microbial communities from different depths in the PS reactor. Asterisks indicate that the encapsulation of bacteria in the calcified pellet matrix hampered DNA extraction from the 5-m and 6-m samples. (B) Pearson similarities of the samples from the different depths to the sample from the 1st meter.

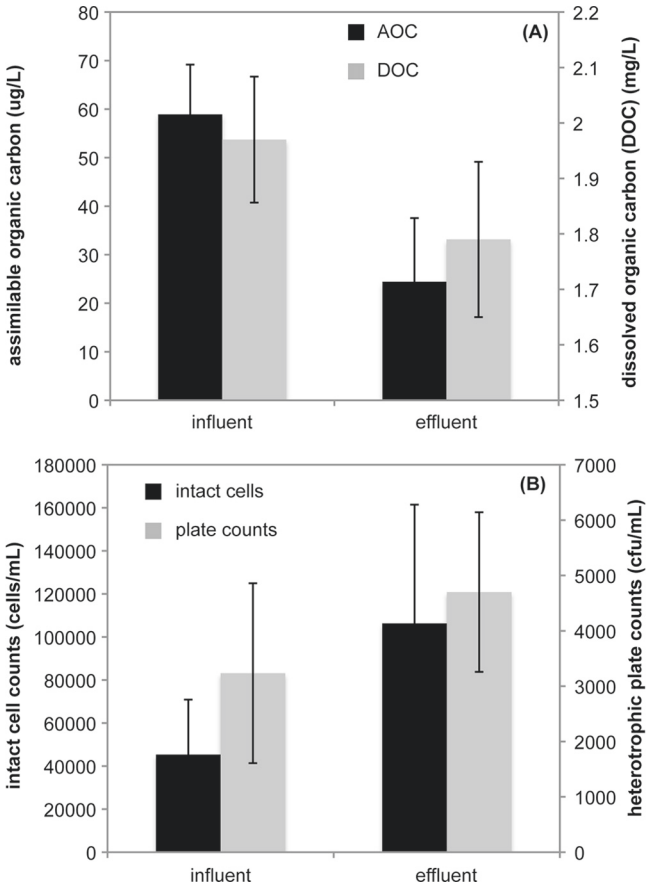

FIG. 5. Changes in organic carbon and microbial content of the water due to the PS process. (A) Concentrations of assimilable and dissolved organic carbon (AOC and DOC, respectively). (B) Intact cells measured by flow cytometry and conventional heterotrophic plate counts. Data points are mean values for triplicate samples taken on three separate days. Error bars indicate standard deviations.

the reactor are not entirely surprising; although dynamic changes occur through the reactor (Fig. 2), the sampling points do not represent defined layers. Indeed, if the similarities of all the samples are considered, an overall Pearson similarity of almost 90% is found, which is very high. In fact, all pellets progress gradually from the top of the reactor downward, and bacteria are continuously and irreversibly captured in the calcite matrix (Fig. 3E). This was also observed by determining the similarities between the 1-m sample and the samples from the other depths (Fig. 4B). Moreover, the high flow rates and relatively small pH changes in the high-activity sections of the reactor (0 to 5 m) mean that almost no specific stratification can be expected in the PS reactor. Also, due to the high flow rates, any suspended/detached bacteria from the lower sections of the reactor are rapidly transported to the top, either alone or attached to small, loose calcite flocs that could be seen in the water phase (data not shown), thus initiating the colonization of the newly introduced sand particles.

Functional contribution of bacteria in PS reactors. The presence of a high biomass concentration in the PS reactors has direct consequences for water quality and for the overall performance of the treatment system. Previous analysis of DOC and natural organic matter (NOM) fractions has revealed that only a small amount of organic carbon (about 6% of influent DOC; 315 μg/liter) is removed in a PS reactor and that the removed DOC comprises all fractions identified in a size exclusion chromatogram (1). Chen and coworkers (5) have suggested that any organic carbon removal in PS reactors could be attributed to abiotic coprecipitation with calcite, a plausible event that has been described previously (20, 15) and that cannot be ruled out in the present study. However, analysis of AOC concentrations before and after pellet softening shows that a relatively large fraction (about 11%; 35 μg/liter) of the DOC that was removed was in the form of AOC (Fig. 5A). Importantly, this constitutes a removal of 60% of the AOC that is produced during ozonation. Taking this finding together with the presence of a large quantity of viable bacterial cells in the reactor, which can persist and multiply only through the continuous consumption of significant quantities of biologically available nutrients, one can assume that bacterial growth contributes significantly to carbon removal in the PS reactors. AOC has often been described as one of the essential parameters for ensuring the biological stability of drinking water (12, 26), and waterworks in the Netherlands typically aim at AOC removal to levels below 10 μg/liter (26). In this respect, the removal of more than 50% of the AOC is definitely complementary to the treatment process and contributes to the overall goal of achieving biologically stable drinking water. In an overview of operation at a Dutch treatment plant using PS reactors, Tapia et al. (24) discussed the alternative option of using abiotic nanofiltration instead of conventional PS reactors in the future design of softening reactors. In this respect, it should be

considered that AOC passes through nanofiltration membranes (7), and even though this process is still followed by BAC filtration in the treatment system, the BAC filters would sustain an additional organic carbon burden, which might alter operation performance and ultimately water quality. Furthermore, high concentrations of AOC may cause strong membrane fouling, requiring more effort for process maintenance.

The majority of the biomass that is present on the pellets is eventually captured completely in the calcite matrix (Fig. 3E) and is removed as a reusable product (28). However, a small fraction of bacteria (average from three samples, 0.6×10^5 cells/ml) is also continuously detached and released from the reactor, a process measurable as an increase in the concentration of intact cells after softening (Fig. 5B). This concentration is similar to cell concentrations measured in the effluents of conventional drinking water biofiltration systems (11, 12). Flow cytometry suggests that the suspended/detached cells are large cells, corresponding to the filamentous organisms seen on the pellets (data not shown). The size of the cells may also be indicative of fast exponential growth occurring in the PS reactors. Also, a notable increase in the concentration of cultivable bacteria in the reactor effluent was observed, although this value was about an order of magnitude lower than the concentration of intact cells (Fig. 5B). While there is no reason to view these detached bacteria as malignant, their presence has to be taken into account when downstream processes are considered (e.g., potential impact on GAC filters or the need for post-treatment disinfection). Moreover, it has been observed for these reactors that operation at low temperatures (<5°C) often resulted in considerable increases in the concentrations of cultivable bacteria, probably ascribable to altered hydraulic conditions (M. Dignum, unpublished data).

Potential problems with biomass in PS reactors. High biomass concentrations in the PS reactors may also contribute to unforeseen operational problems. Excessive filamentous growth is a known problem in activated-sludge systems, resulting in bulking sludge and numerous well-described problems with sludge settling (21). Disturbance layers, characterized by fluffy, cauliflower-like $CaCO_3$ particles and adverse reactor behavior (e.g., reduced crystallization), have been detected previously during routine sampling of PS reactors, requiring intensive manual removal of the sludge/pellets (E. Baars, personal communication). Figure 3F shows a representative SEM image of particles from such a layer, sampled from another treatment plant in the Netherlands (Weesperkarspel; Amsterdam), where the problem of disturbance layers in PS reactors is known to occur. The presence of a large quantity of filamentous bacteria and the absence of organized crystallization structures are evident. While the specific role of bacteria in the formation of these disturbance layers is not known, it is clear that their presence contributes to the bulking nature of the disturbance layer. Additional research on the microbiological factors involved in the bulking phenomenon (e.g., community composition and specific growth conditions) might aid in future operation and control strategies.

Conclusions. We have shown that centralized drinking water PS reactors, preceded by an oxidation step, are opportunistically colonized at high densities by a diverse bacterial community. These organisms proliferate in the presence of highly biodegradable nutrients in the water after ozonation, as soon as the pH in the water is neutralized as a result of calcite crystallization. The colonizing bacteria contribute actively to the drinking water treatment process by the removal of a considerable amount of assimilable organic carbon, enhancing the biological stability of the water. However, there is evidence to suggest that excessive bacterial growth can contribute to the establishment of problematic "disturbance layers" in PS reactors. Finally, most of the biomass in normally operating PS reactors is irreversibly captured in the calcite matrix and is eventually removed from the reactors together with the pellets as a reusable product.

ACKNOWLEDGMENTS

Research on this project was financially supported by the 6th Framework European integrated project TECHNEAU (018320) and by project grant G.0808.10N from the Research Foundation of Flanders (FWO).

K. Marquard (UniZH), B. Kratochvil (IRIS, ETH), and M. Peter (Eawag) contributed to the SEM and CLSM images. E. Baars (Waternet) assisted with the sampling. K. van Schagen assisted with the reactor modeling.

REFERENCES

1. **Baghoth, S. A., M. Dignum, A. Grefte, J. Kroesbergen, and G. L. Amy.** 2009. Characterisation of NOM in a drinking water treatment process train with no disinfectant residual. Water Sci. Technol. **9:**379–386.
2. **Berney, M., et al.** 2008. Rapid, cultivation-independent assessment of microbial viability in drinking water. Water Res. **42:**4010–4018.
3. **Boon, N., W. De Windt, W. Verstraete, and E. M. Top.** 2002. Evaluation of nested PCR-DGGE (denaturing gradient gel electrophoresis) with group-specific 16S rRNA primers for the analysis of bacterial communities from different wastewater treatment plants. FEMS Microbiol. Ecol. **39:**101–112.
4. **Boon, N., J. Goris, P. De Vos, W. Verstraete, and E. M. Top.** 2000. Bioaugmentation of activated sludge by an indigenous 3-chloroaniline-degrading *Comamonas testosteroni* strain, I2gfp. Appl. Environ. Microbiol. **66:**2906–2913.
5. **Chen, Y.-H., H.-H. Yeh, M.-C. Tsai, and W. L. Lai.** 2000. The application of fluidized bed crystallization in drinking water softening. J. Chin. Inst. Environ. Eng. **10:**177–184.
6. **Chien, C. C., C. M. Kao, C. W. Chen, C. D. Dong, and C. Y. Wu.** 2008. Application of biofiltration system on AOC removal: column and field studies. Chemosphere **71:**1786–1793.
7. **Escobar, I. C., S. Hong, and A. A. Randall.** 2000. Removal of assimilable organic carbon and biodegradable dissolved organic carbon by reverse osmosis and nanofiltration membranes. J. Membrane Sci. **175:**1–17.
8. **Ferris, F. G., W. S. Fyfe, and T. J. Beveridge.** 1987. Bacteria as nucleation sites for authentic minerals in a metal-contaminated lake sediment. Chem. Geol. **63:**225–232.
9. **Graveland, A., J. C. van Dijk, P. J. de Moel, and J. H. C. M. Oomen.** 1983. Developments in water softening by means of pellet reactors. J. Am. Water Works Assoc. **77:**616.
10. **Hammes, F., N. Boon, J. de Villiers, W. Verstraete, and S. D. Siciliano.** 2003. Strain-specific ureolytic microbial calcium carbonate precipitation. Appl. Environ. Microbiol. **69:**4901–4909.
11. **Hammes, F., et al.** 2008. Flow-cytometric total bacterial cell counts as a descriptive microbiological parameter for drinking water treatment processes. Water Res. **42:**269–277.
12. **Hammes, F., C. Berger, O. Köster, and T. Egli.** 2010. Biological stability of drinking water without disinfectant residuals: a case-study of the Zürich water supply system. J. Water Supply Res. Technol. AQUA **59:**31–40.
13. **Hsu, B.-M., and H.-H. Yeh.** 2003. Removal of *Giardia* and *Cryptosporidium* in drinking water treatment: a pilot-scale study. Water Res. **37:**1111–1117.
14. **Karl, D. M.** 1980. Cellular nucleotide measurements and applications in microbial ecology. Microbiol. Rev. **44:**739–796.
15. **Li, C.-W., J.-C. Liao, and Y.-C. Lin.** 2005. Integrating a membrane and a fluidized pellet reactor for removing hardness: effects of NOM and phosphate. Desalination **175:**279–288.
16. **Magic-Knezev, A., and D. van der Kooij.** 2004. Optimisation and significance of ATP analysis for measuring active biomass in granular activated carbon filters used in water treatment. Water Res. **38:**3971–3979.
17. **Marzorati, M., L. Wittebolle, N. Boon, D. Daffonchio, and W. Verstraete.** 2008. How to get more out of molecular fingerprints: practical tools for microbial ecology. Environ. Microbiol. **10:**1571–1581.
18. **Muyzer, G., E. C. de Waal, and A. G. Uitterlinden.** 1993. Profiling of complex microbial populations by denaturing gradient gel electrophoresis analysis of

polymerase chain reaction-amplified genes coding for 16S rRNA. Appl. Environ. Microbiol. **59:**695–700.
19. **Peter-Varbanets, M., F. Hammes, M. Vital, and W. Pronk.** 2010. Stabilization of flux during dead-end ultra-low pressure ultrafiltration. Water Res. **44:**3607–3616.
20. **Schäfer, A. I., A. G. Fane, and T. D. Waite.** 1998. Nanofiltration of natural organic matter: removal, fouling and the influence of multivalent ions. Desalination **118:**109–122.
21. **Seka, A. M., T. van de Wiele, and W. Verstraete.** 2001. Feasibility of a multi-component additive for efficient control of activated sludge filamentous bulking. Water Res. **35:**2995–3003.
22. **Shi, B., and J. S. Taylor.** 2007. Iron and copper release in drinking-water distribution systems. J. Environ. Health **70:**29–36.
23. **Southam, G.** 2000. Bacterial surface-mediated mineral formation, p. 257–276. *In* D. R. Lovley (ed.), Environmental microbe-metal interactions. ASM Press, Washington, DC.
24. **Tapia, M., M. A. Siebel, A. W. C. van der Helm, E. T. Baars, and H. J. Gijzen.** 2008. Environmental, financial and quality assessment of drinking water processes at Waternet. J. Clean. Prod. **16:**401–409.
25. **Urfer, D., P. M. Huck, S. D. J. Booth, and B. M. Coffey.** 1997. Biological filtration for BOM and particle removal: a critical review. J. Am. Water Works Assoc. **89:**83–98.
26. **van der Kooij, D.** 1992. Assimilable organic carbon as an indicator of bacterial regrowth. J. Am. Water Works Assoc. **84:**57–65.
27. **van der Veen, C., and A. Graveland.** 1988. Central softening by crystallization in a fluidized-bed process. J. Am. Water Works Assoc. **80:**51–58.
28. **van Dijk, J. C., and D. A. Wilms.** 1991. Water treatment without waste material—fundamentals and state of the art of pellet softening. J. Water Supply Res. Technol. AQUA **40:**263–280.
29. **van Schagen, K., R. Babuška, L. Rietveld, and E. T. Baars.** 2006. Optimal flow over multiple parallel pellet reactors: a model-based approach. Water Sci. Technol. **53:**493–501.
30. **van Schagen, K., L. Rietveld, and R. Babuška.** 2008. Dynamic modelling for optimisation of pellet softening. J. Water Supply Res. Technol. AQUA **57:**45–56.
31. **van Schagen, K., L. Rietveld, R. Babuška, and E. Baars.** 2008. Control of the fluidised bed in the pellet softening process. Chem. Eng. Sci. **63:**1390–1400.
32. **Velten, S., F. Hammes, M. Boller, and T. Egli.** 2007. Rapid and direct estimation of active biomass on granular-activated carbon through adenosine tri-phosphate (ATP) determination. Water Res. **41:**1973–1983.
33. **Wittebolle, L., et al.** 2009. Initial community evenness favours functionality under selective stress. Nature **458:**623–626.
34. **Yavich, A. A., K. H. Lee, K. C. Chen, L. Pape, and S. J. Masten.** 2004. Evaluation of biodegradability of NOM after ozonation. Water Res. **38:** 2839–2846.